



**HAL**  
open science

## Mesoscale and local scale evaluations of quantitative precipitation estimates by weather radar products during a heavy rainfall event.

Basile Pauthier, Benjamin Bois, Thierry Castel, D. Thévenin, Carmela Chateau Smith, Yves Richard

► **To cite this version:**

Basile Pauthier, Benjamin Bois, Thierry Castel, D. Thévenin, Carmela Chateau Smith, et al.. Mesoscale and local scale evaluations of quantitative precipitation estimates by weather radar products during a heavy rainfall event.. *Advances in Meteorology*, 2016, 2016, pp.6089319. 10.1155/2016/6089319 . hal-01385646

**HAL Id: hal-01385646**

**<https://hal.science/hal-01385646>**

Submitted on 21 Feb 2024

**HAL** is a multi-disciplinary open access archive for the deposit and dissemination of scientific research documents, whether they are published or not. The documents may come from teaching and research institutions in France or abroad, or from public or private research centers.

L'archive ouverte pluridisciplinaire **HAL**, est destinée au dépôt et à la diffusion de documents scientifiques de niveau recherche, publiés ou non, émanant des établissements d'enseignement et de recherche français ou étrangers, des laboratoires publics ou privés.

## Research Article

# Mesoscale and Local Scale Evaluations of Quantitative Precipitation Estimates by Weather Radar Products during a Heavy Rainfall Event

Basile Pauthier,<sup>1</sup> Benjamin Bois,<sup>1</sup> Thierry Castel,<sup>1</sup> D. Thévenin,<sup>2</sup> Carmela Chateau Smith,<sup>3</sup> and Yves Richard<sup>1</sup>

<sup>1</sup>Centre de Recherche de Climatologie, Biogéosciences UMR 6282 CNRS, Université Bourgogne Franche-Comté, 6 bd Gabriel, 21000 Dijon, France

<sup>2</sup>Météo-France Direction Régionale Centre-Est, 22 rue Louis de Broglie, 21000 Dijon, France

<sup>3</sup>UFR SVTE, Université Bourgogne Franche-Comté, 6 bd Gabriel, 21000 Dijon, France

Correspondence should be addressed to Basile Pauthier; [basile.pauthier@u-bourgogne.fr](mailto:basile.pauthier@u-bourgogne.fr)

Received 8 June 2016; Revised 9 September 2016; Accepted 19 September 2016

Academic Editor: Bin Yong

Copyright © 2016 Basile Pauthier et al. This is an open access article distributed under the Creative Commons Attribution License, which permits unrestricted use, distribution, and reproduction in any medium, provided the original work is properly cited.

A 24-hour heavy rainfall event occurred in northeastern France from November 3 to 4, 2014. The accuracy of the quantitative precipitation estimation (QPE) by PANTHERE and ANTILOPE radar-based gridded products during this particular event, is examined at both mesoscale and local scale, in comparison with two reference rain-gauge networks. Mesoscale accuracy was assessed for the total rainfall accumulated during the 24-hour event, using the Météo France operational rain-gauge network. Local scale accuracy was assessed for both total event rainfall and hourly rainfall accumulations, using the recently developed HydraVitis high-resolution rain gauge network. Evaluation shows that (1) PANTHERE radar-based QPE underestimates rainfall fields at mesoscale and local scale; (2) both PANTHERE and ANTILOPE successfully reproduced the spatial variability of rainfall at local scale; (3) PANTHERE underestimates can be significantly improved at local scale by merging these data with rain gauge data interpolation (i.e., ANTILOPE). This study provides a preliminary evaluation of radar-based QPE at local scale, suggesting that merged products are invaluable for applications at very high resolution. The results obtained underline the importance of using high-density rain-gauge networks to obtain information at high spatial and temporal resolution, for better understanding of local rainfall variation, to calibrate remotely sensed rainfall products.

## 1. Introduction

Accurate Quantitative Precipitation Estimation (QPE) is necessary at various spatial and temporal scales [1, 2]. Heavy rainfall events are expected to increase during the twenty-first century [3]. Better monitoring and prediction of such events and their consequences are of primary importance for hydrology (the hydrological rainfall-runoff relationship during flash floods [4–8]), particularly in mountainous regions [9, 10], for sustainable agriculture [11], and for urban planning [12–16]. National meteorological networks are generally not dense enough to fully document local scale rainfall estimates.

New-generation high-resolution weather radar systems offer opportunities to detect heavy rainfall events with applications for many domains, such as nowcasting, climatology, hydrology, and agriculture [17]. During the last decade, various countries have deployed a number of major technological evolutions (e.g., Doppler and dual-polarization), in addition to the densification of their radar networks (e.g., ARAMIS in France or NEXRAD in the USA). All radar-based rainfall estimates share the same basic physical principles (see pioneering work by Marshall et al. in 1947 [18]), thus requiring correction and calibration, which remains a challenging issue [19, 20]. Rainfall rate ( $R$ ) is estimated

using the conventional  $Z$ - $R$  relationship. The coefficients of the  $Z$ - $R$  relationship [18, 21–24] are related to the drop-size distribution (DSD).

Despite the use of the dual-polarization technique, signal attenuation during heavy rainfall may induce underestimation, especially for X- and C-band radar, the radars most frequently used in France [25, 26]. To prevent excessive underestimation, it is necessary to integrate rain gauge measurements for attenuation correction and empirical adjustment [17, 27–30].

The potential value of new-generation high-resolution weather radar systems for QPE has been evaluated and used in recent studies [2, 31–34]. Despite encouraging results for rainfall estimation and its application at mesoscale (10–500 km [35]), the quality of radar rainfall estimates may vary greatly, in relation to (1) the coefficient applied for attenuation correction, that is, calibration of the changing  $Z$ - $R$  relationship; (2) the location and size of heavy rainfall events; (3) the density of the rain gauge network used to compute the single-bias adjustment factor and to generate products merging radar rainfall with interpolated rain gauge data. With regard to attenuation correction, a new polarimetric processing chain provides improved rainfall estimates (e.g., [32]).

Rainfall event characteristics and network density must both be taken into account in rainfall estimates [36]. The location and size of rainfall events at mesoscale, together with bias adjustment factors and merged product construction, are usually based on data from mesoscale national rain gauge networks. Radar-based QPE has generally been evaluated using networks of similar density (e.g., [34, 37]), but few robust estimates exist at local scale (0.1 m–50 km [35]). Rain gauges are generally not deployed in sufficient density on hilly terrain or in remote locations. The HydraVitis rain gauge network, recently installed in Burgundy, northeastern France (45 rain gauges over 28 km<sup>2</sup> [38]), was designed to capture the spatiotemporal variability of rainfall, particularly the contrasted patterns that may arise at local scale over a complex terrain during heavy rainfall episodes. The density of the HydraVitis network thus provides the opportunity to assess the capability of radar products to document a heavy rainfall event at local scale [39]. In this study, HydraVitis is therefore taken as reference for the capture of rainfall at local scale.

The main aim is to assess the quality of QPE in PAN-THERE and ANTILOPE radar-based products, during a heavy rainfall event. First, total rainfall for the 24-hour event was assessed at both mesoscale and local scale. The second analysis focuses on hourly, local scale rainfall patterns.

In the following sections, the heavy rainfall event occurring on November 3 to 4, 2014, is presented, and the two reference rain gauge network datasets (Météo France and HydraVitis) are described. The main characteristics of the radar products are explained, as is the method for comparing point and gridded products. Finally, the ability of radar products to capture the spatiotemporal variability of the rainfall event is evaluated.

## 2. The Study Event and the Reference Rain Gauge Networks Specifications

This case study is a 24-hour rainfall event, from 9.00 pm on November 3 to 8.00 pm on November 4, 2014. An unstable rainy disturbance was moving slowly southeastward across France, generating strong rainfall accumulations along axis oriented SSW/NNE [40]. Rainfall data for this event were collected at both mesoscale (150 km radius) and local scale (28 km<sup>2</sup>). The interest of this particular event is that the rainy front presented both stratiform and convective particularities [40]. This exceptional event generated the equivalent of a month of rainfall in 24 hours, with accumulations ranging from 70 to 110 mm [41]. Many floods resulted from this event and a state of natural disaster was recognized for 40 towns in the Saône-et-Loire administrative area (“département” in French).

The event of November 3 to 4, 2014, is an interesting case study for high-resolution radar product evaluation because of (1) its nature (both stratiform and convective), making adjustment of the  $Z$ - $R$  relationship challenging; (2) its strong accumulations, which may attenuate the beam; (3) its local spatial variability, which cannot be captured by the low-density national rain gauge network; and (4) its consequences for hydrometeorological, urban, and agricultural questions.

To analyze this event, two rain gauge networks are used. The first is a subset of the national Météo France network, an operational network composed of SPIEA direct reading and automatic tipping-bucket rain gauges. We extracted data collected by 122 Météo France stations, located up to 150 km away from the centroid of the HydraVitis network, to form the subset used in this study, the Météo France rain gauge network (MFRN; Figure 1(a)). The average distance from an MFRN gauge to its nearest neighbor is 14.4 km. One of these rain gauges is located within the study area covered by the high-resolution HydraVitis network.

The second network, HydraVitis, is composed of 45 tipping-bucket rain gauges (RAINEW III, RainWise® Inc.), covering an area of 28 km<sup>2</sup> (Figure 1(b)). Based on Humphrey et al. [42], rain gauge average measurement error ranged from 0.6% to 4.2%, from the lowest (2 mm) to the highest (200 mm) rainfall intensity [38].

The gauge implementation was based on Météo France recommendations, deployed at a minimum distance of four times the height of the nearest obstacle. Each gauge was linked to a Hobo Pendant UA-002-64 event temperature logger (Onset® Corp.). This device records rainfall data every second, with a 0.258 mm resolution. In order to evaluate measurement uncertainty, four gauges were deployed in pairs less than three meters apart. Network implementation and control are detailed in Pauthier et al. [38]. The average distance to the nearest neighboring gauge is 512 m. Figure 2 indicates the main exposure and slope of the study area and the distribution of rain gauge exposure and slope, showing that the HydraVitis rain gauges cover the main terrain features of the study area. Hourly rainfall amounts were calculated for each rain gauge, as density of the HydraVitis network corresponds to the density recommended in Villarini et al. in 2008 [39].

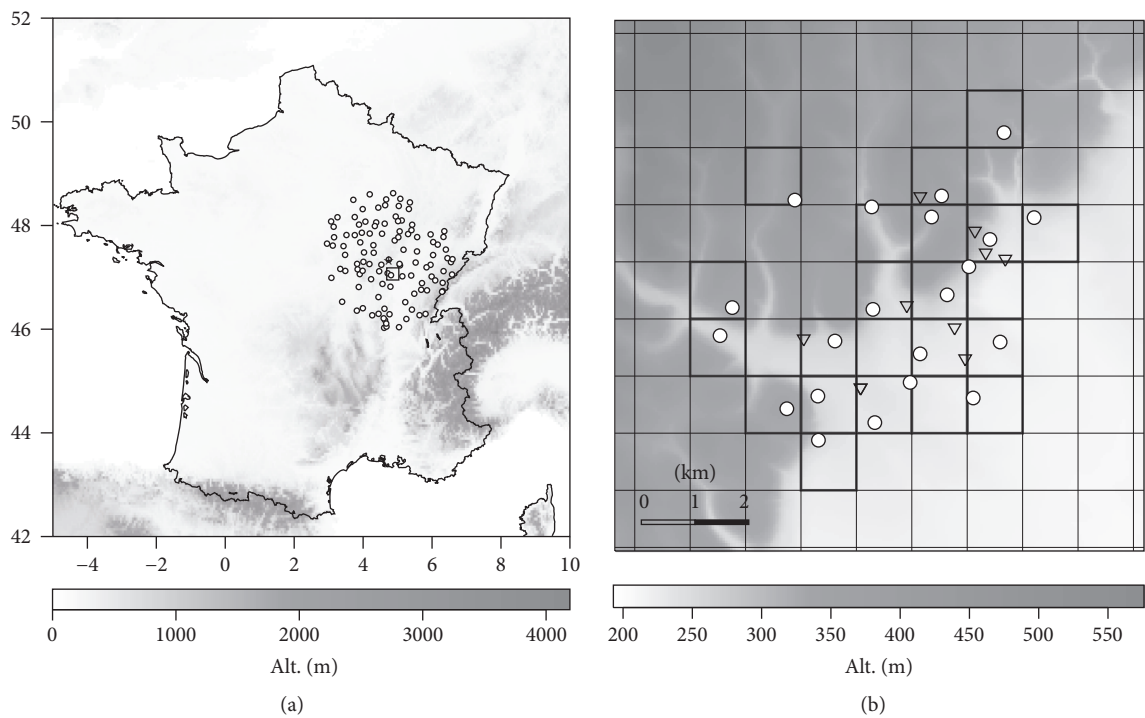


FIGURE 1: The mesoscale and local scale rain gauge network. (a) The star indicates the radar position. Small circles indicate the location of MFRN rain gauges located less than 150 km from the radar. The square indicates the position of the HydraVitis network. (b) White circles indicate the location of the rain gauges providing the HydraVitis data used in this study. The bold gridlines show the boundaries of the 1 km<sup>2</sup> radar pixels in which a rain gauge was available for comparison.

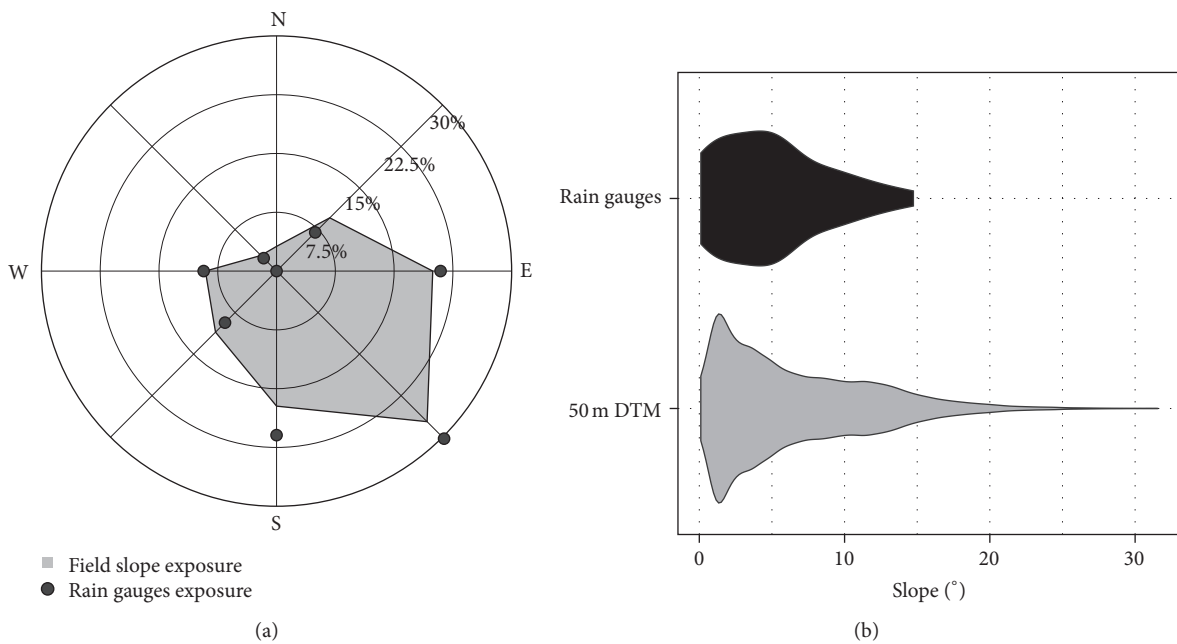


FIGURE 2: (a) Field slope exposure (grey surface) and rain gauge exposure (dark grey points). (b) Slope distribution over the study area. The black zone represents the distribution of HydraVitis rain gauges in relation to topography. The grey zone represents slope distribution for 50 m DTM.

### 3. Radar-Based Products: PANTHERE and ANTILOPE

Two main products derived from weather radar systems are available in France for the monitoring and estimation of rainfall events. The PANTHERE product includes several postprocessing steps aimed at correcting for ground clutter, partial beam blocking, Vertical Profile of Reflectivity (VPR) effects, and synchronisation of radar measurements (see [37] for a full description of the radar processing procedure). In this study, PANTHERE was applied to data collected by the closest radar system, located 31 km north of the HydraVitis network (Figure 1(a), Blaisy-Haut, 47.355278°N 4.775833°E). This radar is equipped with a dual-polarized C-band antenna. Over the study area, the radar signal benefits from low beam blocking at 0.5° (the maximum beam blockage is systematically under 5%).

The PANTHERE product has a 1 km<sup>2</sup> resolution and is computed to provide 5-minute time step rainfall fields. In this study, PANTHERE data were aggregated with an hourly time step.

In order to overcome any difficulty in inferring realistic rainfall amounts, particularly in convective situations, a composite product merging radar-based and rain gauge rainfall is also available. It adjusts PANTHERE estimates by means of *post hoc* integration of kriged data from the Météo France rain gauge network. This corrected product, recently developed by Météo France, is called ANTILOPE [43, 44]. The ANTILOPE data are available at the same time step and spatial resolution as PANTHERE and were also aggregated at an hourly time step in this study.

### 4. Method for Comparing Networks and Gridded Products

The PANTHERE and ANTILOPE radar products (pixel grids) were compared with the MFRN and HydraVitis rain gauge networks (points) at two different scales. For mesoscale comparison, the 122 MFRN 24-hour cumulated rainfall measurement points were individually compared to the relevant PANTHERE QPE grid-pixel (Figure 1(a)). As ANTILOPE is partly composed of spatialized MFRN data, this comparison was only conducted on the PANTHERE data to avoid interdataset dependency.

Local scale comparison was based on HydraVitis data. Only one rain gauge measurement point was used for a given grid-pixel; the nearest rain gauge to the pixel center was systematically selected. Data from 21 rain gauges were therefore compared with 21 grid-pixels from each radar product, at an hourly time step (Figure 1(b)).

### 5. Results

**5.1. Whole Event Rainfall Analysis.** Figure 3(a) shows the radar-based 24-hour cumulated PANTHERE QPE (from Nov. 3 at 21:00 to Nov. 4 at 20:00, covering the whole event). The radar-based QPE exhibits a SSW/NNE elongated pattern where precipitation reached up to 85.2 mm in 24 hours,

according to PANTHERE data. Rain gauges at mesoscale are collected up to 129.6 mm, which is significantly higher than the maximum value registered by PANTHERE product. Radar-derived rainfall is underestimated (Figure 3(b)), especially in zones where cumulated rainfall was close to the maximum value (Figure 3(a)). Previous works [45] indicate that as distance increases, radar-based QPE increasingly underestimates high values. In this case, distance from the radar did not strongly affect PANTHERE QPE (i.e., notable underestimates are found at both 30 km and 150 km from the radar). These underestimates may be attributed to greater attenuation of the radar signal with more intense precipitation. Indeed, Figure 3(a) shows that the strongest precipitation coincides with the greatest underestimation. Red dots in Figure 3(b) are the rain gauges located where the radar beam encountered the greatest cumulated quantities of rainfall between radar and rain gauge. For these rain gauges, QPE values are often largely underestimated (up to 51.5 mm). Such attenuation effects have frequently been reported in the literature [17, 27, 46] and have previously been noted as a limitation of the PANTHERE algorithm.

At local scale, PANTHERE systematically underestimates rainfall (Figures 3(c) and 3(d)). Underestimations are homogeneous around the mean bias value (31.2 mm). The Nash criterion (−20.7) confirms this mismatch. The spatial structure of the rainfall is adequately captured by this radar product (Figure 3(d)). The rain gauges receiving the highest amounts of rainfall are located in the grid-pixels with maximum PANTHERE QPE (Pearson correlation coefficient = 0.73).

ANTILOPE, a product merging spatial interpolation of Météo France rain gauge data with radar-based rainfall data, shows better QPE. It only slightly underestimates rainfall (mean bias = −3.2), as captured by HydraVitis rain gauges (Figures 3(e) and 3(f)). Furthermore, ANTILOPE depicts the rainfall field rather successfully at local scale, as supported by the Pearson correlation (0.72) and Nash criterion (0.49) scores.

**5.2. Hourly Time Step Local Analysis.** Radar (PANTHERE) and composite (ANTILOPE) products were compared to values for those rain gauges located closest to each grid point (from 101 to 647 m), within the area covered by the HydraVitis network. Figure 4 describes the hourly evolution of the QPEs (PANTHERE and ANTILOPE) against rain gauge *in situ* measurements.

Over the 24-hour period, PANTHERE values are underestimated from 0:00 to 6 am, when rainfall intensities were highest. The spatial variability is adequately reproduced for only a few hours (1:00, 2:00, and 7:00 am).

The ability of the composite product, ANTILOPE, to reduce the PANTHERE biases is confirmed at the hourly time scale. The ANTILOPE QPE values are almost systematically closer to rain gauge values than to PANTHERE estimates. For hours when rain gauges show a spatial structure, the ANTILOPE QPE retrieves this structure at least as well as PANTHERE.

Figure 5(a) presents hourly rainfall records averages for radar-derived products and rain gauges. Rainfall intensities

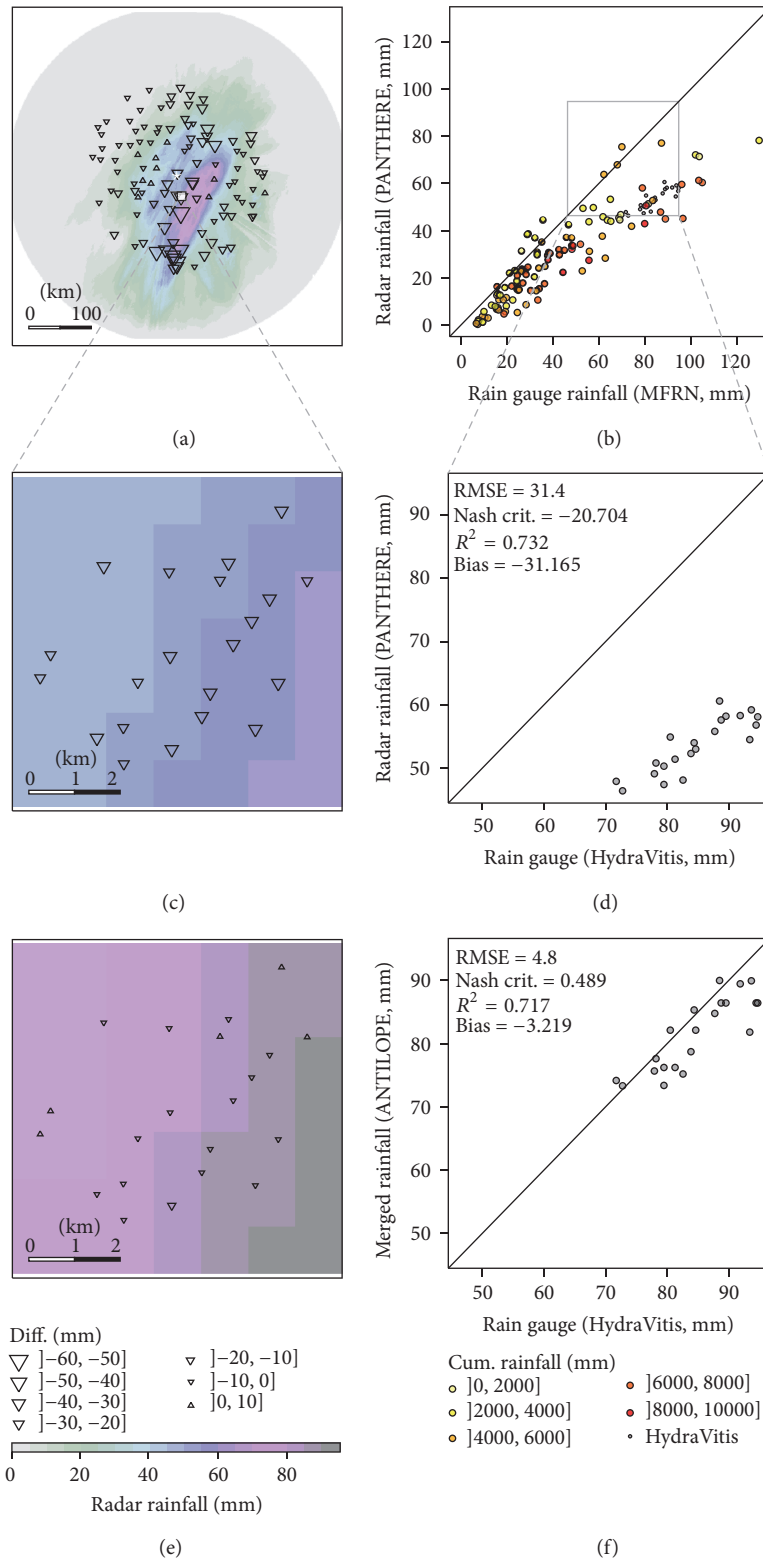


FIGURE 3: Comparison of 24-hour cumulated rainfall values from radar (PANTHERE) and rain gauges, from Nov. 3 at 21:00 to Nov. 4 at 20:00. (a) Radar rainfall map. The white star indicates the radar position and the white square indicates the HydraVitis network position. Triangle size (MFRN rain gauges) is proportional to the difference between values for radar and rain gauges; inverted triangles represent underestimated values; the regular triangles represent accurate or slightly overestimated values. (b) Scatterplot comparing PANTHERE to rain gauge rainfall data. Points are colored according to the rainfall summed for all pixels between the radar and each rain gauge (source of potential attenuation effect). (c) Zoom of (a) over the HydraVitis local scale rain gauge network. Triangle size (HydraVitis rain gauges) is proportional to the difference between values for radar and rain gauges. (d) Scatterplot comparing PANTHERE to rain gauge rainfall data. ((e) and (f)) The same as (c) and (d), respectively, but using the merged radar-based/MFRN rain gauge ANTILOPE data, instead of PANTHERE radar data.

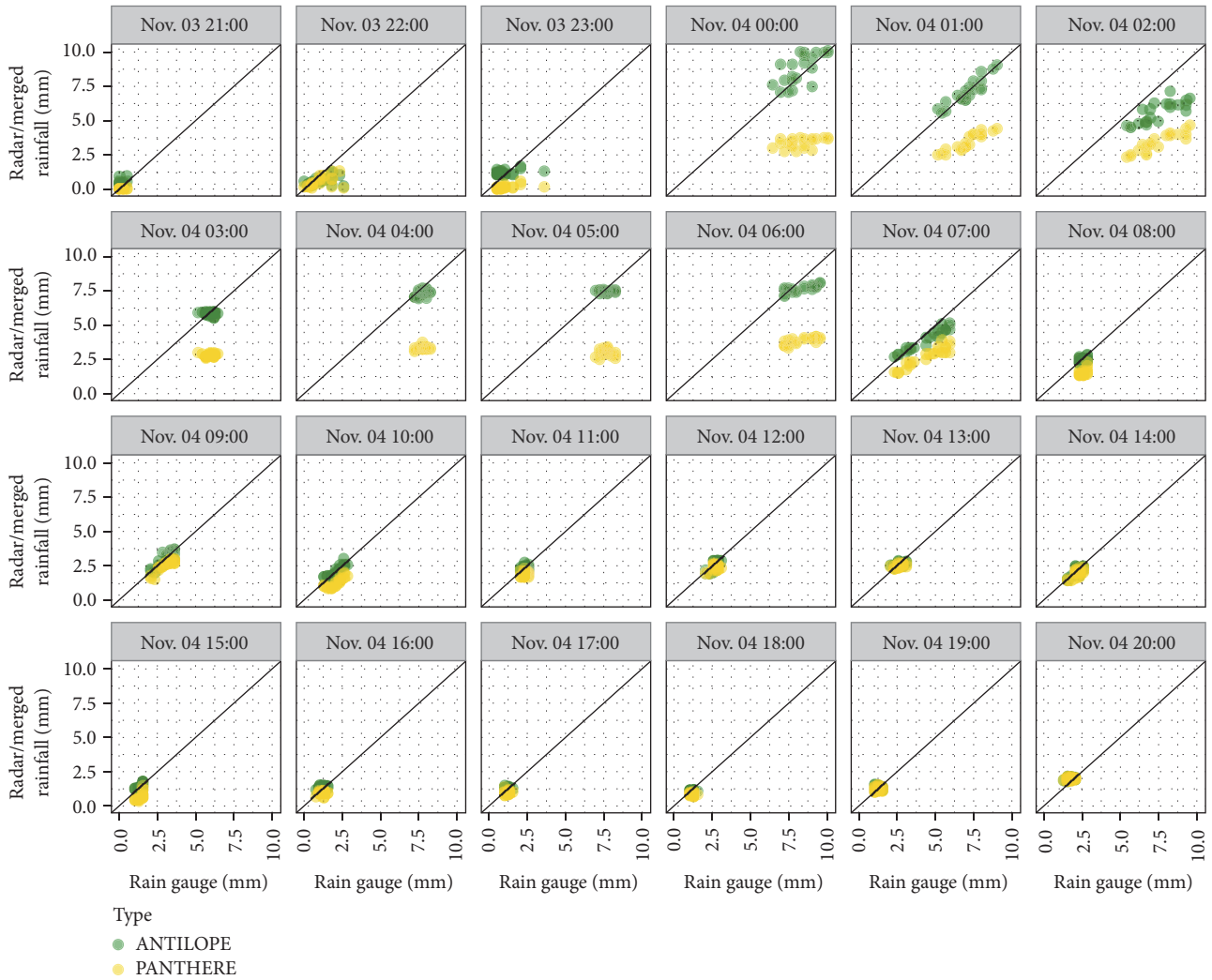


FIGURE 4: Hourly comparison between grid-pixels for PANTHERE and ANTILOPE radar products and HydraVitis rain gauges.

(mm/h) increase sharply at 0:00 on Nov. 4 to 8.3 mm/h (rain gauge average). From 0:00 to 2:00, rainfall spatial variability is at its maximum (rain gauge standard deviation, vertical blue bars in Figure 5(a), from 1.03 to 1.3 mm/h). From 3:00 to 5:00, hourly rainfall remains high (5.9 to 7.7 mm/h) but is rather homogeneous in space (standard deviations from 0.31 to 0.38 mm/h). At 6:00, rainfall intensity rises to 8.3 mm/h (rain gauges average) with a strong spatial variability and decreases from 4 to 2 mm/h approximately, until 13:00 (i.e., 1 pm), with little spatial variation at local scale (standard deviations ranging from 0.18 to 0.51 mm/h during this period). Rainfall finally falls to about 1.5 mm/h after 15:00. Intensities are homogenous in space throughout the study area (standard deviation from 0.18 to 0.22 mm/h).

PANTHERE QPE is almost systematically underestimated during the whole period (except rainfall from 19:00 and 20:00 on Nov. 4; Figure 5(b)). From midnight to 6:00 on November 4, PANTHERE underestimated hourly rainfall rates (3–5 mm), while rain gauge values were almost twice as high (5–9 mm). This underestimation can be linked to

fluctuations in the Z-R relationship, calibration biases, or signal attenuation due to stronger rainfall between the radar site and the study zone [37].

The ANTILOPE QPE provided limited bias (Figure 5(b); mean bias =  $-0.13$  mm/h). The largest underestimation is at 2:00 on Nov. 4 (bias =  $-1.88$  mm/h). Both radar-based QPEs provide spatially consistent hourly precipitation fields (though largely underestimated for PANTHERE) compared to rain gauge data, in many cases. PANTHERE is significantly correlated (Figure 5(c)) with rain gauge data during the whole event but not from 3:00 to 5:00, at 11:00, and from 16:00 to 20:00 on November 4. The ANTILOPE hourly rainfall correlations are also not significant during the first 3 hours of the event. ANTILOPE provides very accurate hourly rainfall fields at local scale, at 1:00, 7:00, 9:00, and 10:00 am on November 4 (Nash criteria equal to 0.843, 0.706, 0.721, and 0.778, resp., Figure 5(d)).

Because PANTHERE underestimates precipitation, a good match to rain gauges is never observed (Nash criterion is always below 0, which is not considered as satisfactory,

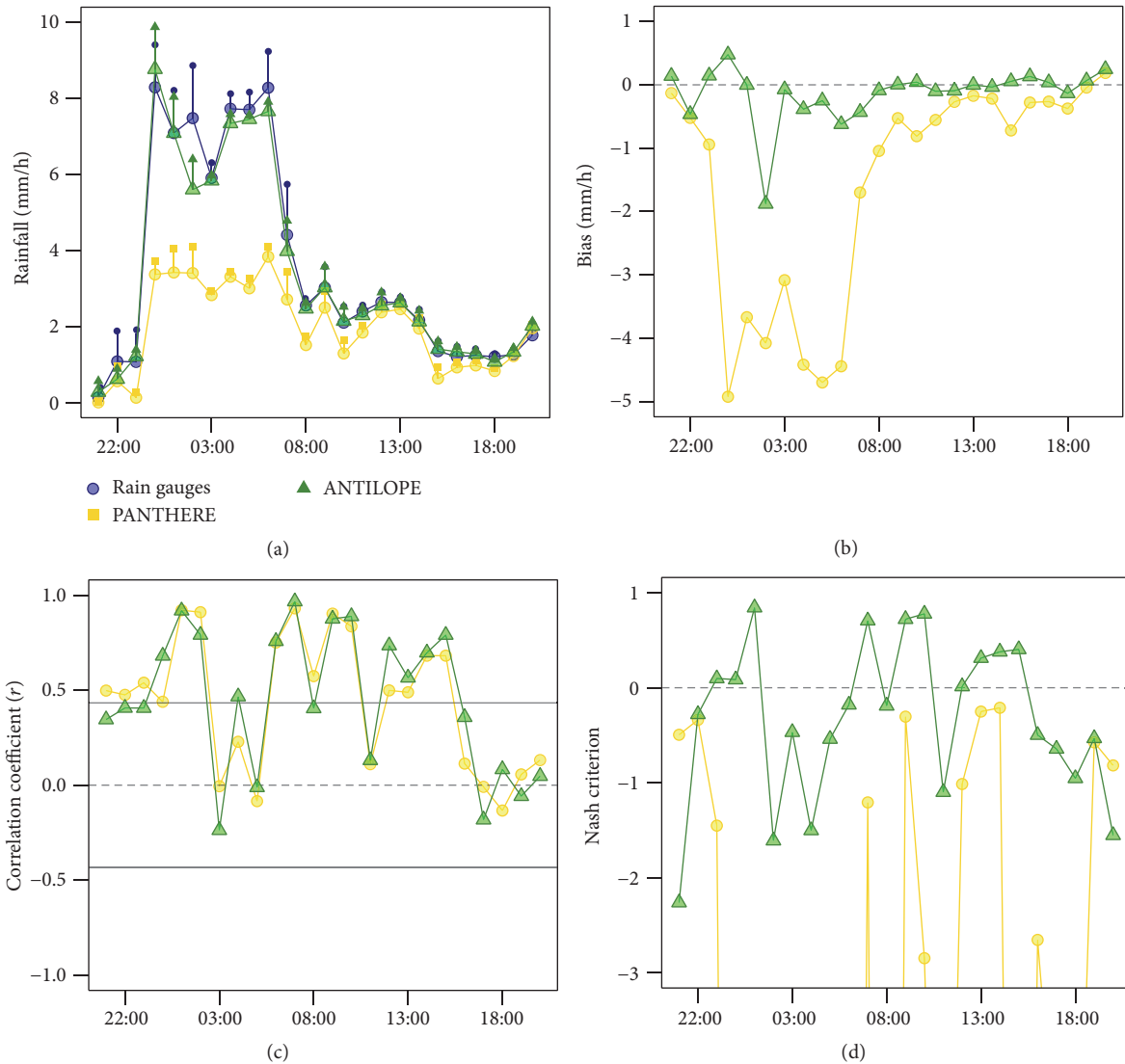


FIGURE 5: Hourly statistics for radar-derived products and HydraVitis rain gauges ( $N = 21$  pixels/rain gauges). (a) Hourly rainfall averaged for 21 pixels (rain gauges) at local scale. Vertical bars indicate the standard deviation (i.e., spatial variability). (b) The mean difference between radar-derived products and rain gauges. (c) Pearson correlation coefficients. The solid grey horizontal lines indicate the value corresponding to statistically significant  $r$  (Student dist.,  $p$  value = 5%). (d) Nash criterion. Light green triangles and yellow circles, respectively, represent ANTILOPE and PANTHERE products.

following [47]), despite good correlation with rain gauges (e.g., at 7:00 Nov. 4; Figure 5).

## 6. Discussion and Conclusion

This study analyzed the performance of two operational radar-derived products in Northern France, during a long, heavy rainfall event that resulted in flooding and heavy damage. The analysis of this event corroborates previous evaluations of radar rainfall and provides novel results regarding the capacity of radar products to capture the spatial variability of rainfall at mesoscale and more particularly at local scale. This analysis confirms the relevance of these products for hydrological modelling, real-time flood assessment,

and water management for agriculture at the farm level, for example. Our main findings at hourly scale supported by 24 patterns are summed up and discussed hereafter.

(a) Despite considerable improvement in radar technology and algorithms, radar QPE fails to estimate rainfall fields accurately at mesoscale for such events. Although, in our study, the PANTHERE cumulated QPE spatial pattern is similar to that of rain gauges, the strong underestimation makes this product unreliable for meteorological, hydrological, or agricultural applications. The long sought-after goal of using radar rainfall data to replace costly rain gauge networks for rainfall measurement has not yet been attained. Even so, considerable improvements have been made



through the decades [48]; since its first applications [18], the use of mesoscale rain gauge networks to readjust radar rainfall is still required to provide satisfactory QPE [2, 49]. Our results clearly corroborate these previous observations.

- (b) It is possible to reduce underestimation by merging interpolated mesoscale rain gauge data with radar QPE, as in the ANTILOPE product [43, 44]. Such merging provides useful products to estimate hourly QPE fields at local scale, even in situations where considerable attenuation is expected. Hourly precipitation data from the HydraVitis network are well correlated with both radar and merged products. High-resolution rainfall fields are crucial for hydrological applications, especially flood event prediction. Composite products, such as ANTILOPE, provide a viable alternative to high-density rain gauge networks, which are practically and financially difficult to deploy and exploit. Careful consideration of the quality and representativeness of the rain gauge network should be considered in conjunction with refinements to mathematical techniques when developing rain gauge radar merging products [36].
- (c) Improving radar rainfall products requires high density and quality ground data for validation [48, 50]. The HydraVitis network (currently composed of 45 rain gauges from 2 m to 6 km apart) aims to provide reliable information about local spatiotemporal variation in rainfall and thus help to improve remotely sensed rainfall products. The two-year dataset recorded by the HydraVitis network (2014–2016) offers the opportunity to statistically assess and quantify these preliminary results in the near future.

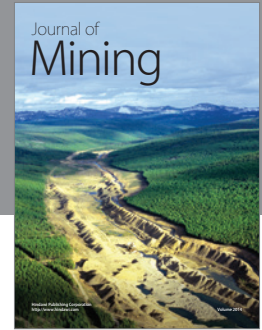
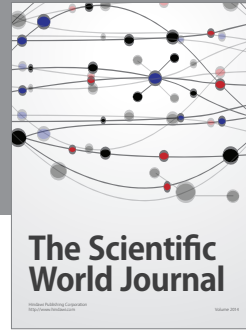
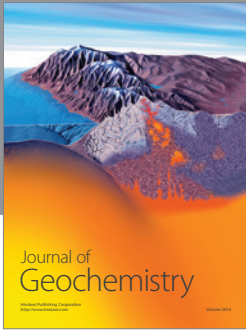
## Competing Interests

The authors declare that they have no competing interests.

## References

- [1] S. V. Vasiloff, D.-J. Seo, K. W. Howard et al., “Improving QPE and very short term QPF: an initiative for a community-wide integrated approach,” *Bulletin of the American Meteorological Society*, vol. 88, no. 12, pp. 1899–1911, 2007.
- [2] E. Goudenhoofdt and L. Delobbe, “Evaluation of radar-gauge merging methods for quantitative precipitation estimates,” *Hydrology and Earth System Sciences*, vol. 13, no. 2, pp. 195–203, 2009.
- [3] T. F. Stocker, D. Qin, G. K. Plattner et al., *IPCC, 2013: Climate Change 2013: The Physical Science Basis. Contribution of Working Group I to the Fifth Assessment Report of the Intergovernmental Panel on Climate Change*, Cambridge University Press, Cambridge, UK, 2013.
- [4] A. Berne, G. Delrieu, J.-D. Creutin, and C. Obled, “Temporal and spatial resolution of rainfall measurements required for urban hydrology,” *Journal of Hydrology*, vol. 299, no. 3–4, pp. 166–179, 2004.
- [5] E. Gaume, M. Livet, M. Desbordes, and J.-P. Villeneuve, “Hydrological analysis of the river Aude, France, flash flood on 12 and 13 November 1999,” *Journal of Hydrology*, vol. 286, no. 1–4, pp. 135–154, 2004.
- [6] X. He, T. O. Sonnenborg, J. C. Refsgaard, F. Vejen, and K. H. Jensen, “Evaluation of the value of radar QPE data and rain gauge data for hydrological modeling,” *Water Resources Research*, vol. 49, no. 9, pp. 5989–6005, 2013.
- [7] Z. Li, D. Yang, Y. Hong, Y. Qi, and Q. Cao, “Evaluation of radar-based precipitation estimates for flash flood forecasting in the Three Gorges Region,” *Proceedings of the International Association of Hydrological Sciences*, vol. 368, pp. 89–95, 2015.
- [8] A. Rafieenasab, A. Norouzi, S. Kim et al., “Toward high-resolution flash flood prediction in large urban areas—analysis of sensitivity to spatiotemporal resolution of rainfall input and hydrologic modeling,” *Journal of Hydrology*, vol. 531, pp. 370–388, 2015.
- [9] M. Borga, E. N. Anagnostou, and E. Frank, “On the use of real-time radar rainfall estimates for flood prediction in mountainous basins,” *Journal of Geophysical Research Atmospheres*, vol. 105, no. D2, pp. 2269–2280, 2000.
- [10] S. Westrelin, P. Mériaux, S. Dalle, B. Fradon, and G. Jamet, “Déploiement d’un réseau de radars pour anticiper les risques hydrométéorologiques,” *La Météorologie*, vol. 8, no. 83, 11 pages, 2013.
- [11] M. R. Duncan, B. Austin, F. Fabry, and G. L. Austin, “The effect of gauge sampling density on the accuracy of streamflow prediction for rural catchments,” *Journal of Hydrology*, vol. 142, no. 1–4, pp. 445–476, 1993.
- [12] F. Fabry, A. Bellon, M. R. Duncan, and G. L. Austin, “High resolution rainfall measurements by radar for very small basins: the sampling problem reexamined,” *Journal of Hydrology*, vol. 161, no. 1–4, pp. 415–428, 1994.
- [13] T. Einfalt, K. Arnbjerg-Nielsen, C. Golz et al., “Towards a roadmap for use of radar rainfall data in urban drainage,” *Journal of Hydrology*, vol. 299, no. 3–4, pp. 186–202, 2004.
- [14] F. Russo, F. Napolitano, and E. Gorgucci, “Rainfall monitoring systems over an urban area: the city of Rome,” *Hydrological Processes*, vol. 19, no. 5, pp. 1007–1019, 2005.
- [15] F. Renard, *Le risque pluvial en milieu urbain: de la caractérisation de l’aléa à l’évaluation de la vulnérabilité: le cas du Grand Lyon [Ph.D. dissertation]*, Université Jean Moulin Lyon 3, Lyon, France, 2010.
- [16] L.-P. Wang, S. Ochoa-Rodríguez, J. Van Assel et al., “Enhancement of radar rainfall estimates for urban hydrology through optical flow temporal interpolation and Bayesian gauge-based adjustment,” *Journal of Hydrology*, vol. 531, pp. 408–426, 2015.
- [17] P. Tabary, C. Augros, J.-L. Champeaux et al., “Le réseau et les produits radars de Météo-France,” *La Météorologie Rubrique* 83, 2013.
- [18] J. S. Marshall, R. C. Langille, and W. Mc. K. Palmer, “Measurement of rainfall by radar,” *Journal of Meteorology*, vol. 4, no. 6, pp. 186–192, 1947.
- [19] D. Atlas, “Radar calibration: some simple approaches,” *Bulletin of the American Meteorological Society*, vol. 83, no. 9, pp. 1313–1316, 2002.
- [20] P. Tabary, “Efforts to improve the monitoring of the French radar network,” in *Proceedings of the 1st Conference on Radar Meteorology*, pp. 482–485, 2003.
- [21] D. M. A. Jones, “Rainfall drop size-distribution and radar reflectivity,” *Illinois State Water Survey 6*, University of Illinois, Urbana, Ill, USA, 1956.

- [22] A. Sims, "Case studies of areal variations in raindrop size distributions," in *Proceedings of the 11th Radar Weather Conference*, pp. 162–165, American Meteorological Society, Boulder, Colo, USA, 1964.
- [23] H. Sauvageot and J.-P. Lacaux, "The shape of averaged drop size distributions," *Journal of the Atmospheric Sciences*, vol. 52, no. 8, pp. 1070–1083, 1995.
- [24] A. Libertino, P. Allamano, P. Claps, R. Cremonini, and F. Laio, "Radar estimation of intense rainfall rates through adaptive calibration of the Z-R relation," *Atmosphere*, vol. 6, no. 10, pp. 1559–1577, 2015.
- [25] J.-Y. Gu, A. Ryzhkov, P. Zhang et al., "Polarimetric attenuation correction in heavy rain at C band," *Journal of Applied Meteorology and Climatology*, vol. 50, no. 1, pp. 39–58, 2011.
- [26] P. Tabary, A.-A. Boumahmoud, H. Andrieu et al., "Evaluation of two 'integrated' polarimetric Quantitative Precipitation Estimation (QPE) algorithms at C-band," *Journal of Hydrology*, vol. 405, no. 3–4, pp. 248–260, 2011.
- [27] J. J. Gourley, P. Tabary, and J. Parent du Chatelet, "Empirical estimation of attenuation from differential propagation phase measurements at C band," *Journal of Applied Meteorology and Climatology*, vol. 46, no. 3, pp. 306–317, 2007.
- [28] E. N. Anagnostou, M. N. Anagnostou, W. F. Krajewski, A. Kruger, and B. J. Miriovsky, "High-resolution rainfall estimation from X-band polarimetric radar measurements," *Journal of Hydrometeorology*, vol. 5, no. 1, pp. 110–128, 2004.
- [29] M. N. Anagnostou, J. Kalogiros, E. N. Anagnostou, M. Tarolli, A. Papadopoulos, and M. Borga, "Performance evaluation of high-resolution rainfall estimation by X-band dual-polarization radar for flash flood applications in mountainous basins," *Journal of Hydrology*, vol. 394, no. 1–2, pp. 4–16, 2010.
- [30] A. Gires, I. Tchiguirinskaia, D. Schertzer, A. Schellart, A. Berne, and S. Lovejoy, "Influence of small scale rainfall variability on standard comparison tools between radar and rain gauge data," *Atmospheric Research*, vol. 138, pp. 125–138, 2014.
- [31] L. Bouilloud, G. Delrieu, B. Boudevillain, and P.-E. Kirstetter, "Radar rainfall estimation in the context of post-event analysis of flash-flood events," *Journal of Hydrology*, vol. 394, no. 1–2, pp. 17–27, 2010.
- [32] J. F. I. Ventura and P. Tabary, "The new French operational polarimetric radar rainfall rate product," *Journal of Applied Meteorology and Climatology*, vol. 52, no. 8, pp. 1817–1835, 2013.
- [33] C. Birman, F. Karbou, and J.-F. Mahfouf, "Daily rainfall detection and estimation over land using microwave surface emissivities," *Journal of Applied Meteorology and Climatology*, vol. 54, no. 4, pp. 880–895, 2015.
- [34] L. K. Cunha, J. A. Smith, W. F. Krajewski, M. L. Baeck, and B.-C. Seo, "NEXRAD NWS polarimetric precipitation product evaluation for IFloodS," *Journal of Hydrometeorology*, vol. 16, no. 4, pp. 1676–1699, 2015.
- [35] T. R. Oke, *Boundary Layer Climates*, Methuen, London, UK, 1978.
- [36] S. A. Jewell and N. Gaussiat, "An assessment of kriging-based rain-gauge-radar merging techniques," *Quarterly Journal of the Royal Meteorological Society*, vol. 141, no. 691, pp. 2300–2313, 2015.
- [37] P. Tabary, J. Desplats, K. Do Khac, F. Eideliman, C. Gueguen, and J.-C. Heinrich, "The new French operational radar rainfall product. Part II: validation," *Weather and Forecasting*, vol. 22, no. 3, pp. 409–427, 2007.
- [38] B. Pauthier, B. Bois, T. Castel, and Y. Richard, "Note technique d'implantation d'un réseau de pluviomètres en terrain viticole sur la côte de Beaune (France)," *Climatologie*, vol. 11, pp. 34–46, 2014.
- [39] G. Villarini, P. V. Mandapaka, W. F. Krajewski, and R. J. Moore, "Rainfall and sampling uncertainties: a rain gauge perspective," *Journal of Geophysical Research: Atmospheres*, vol. 113, no. D11, 2008.
- [40] Météo France, 2014: bulletin climatique quotidien, [https://donneespubliques.meteofrance.fr/donnees\\_libres/bulletins/BQA/20141103.pdf](https://donneespubliques.meteofrance.fr/donnees_libres/bulletins/BQA/20141103.pdf).
- [41] Météo France, Données climatiques de la station de Dijon, 2016, <http://www.meteofrance.com/climat/france/dijon/21473001/normales>.
- [42] M. Humphrey, J. Istok, J. Lee, J. Hevesi, and A. Flint, "A new method for automated dynamic calibration of tipping-bucket rain gauges," *Journal of the American Meteorological Society*, vol. 14, no. 6, pp. 1513–1519, 1997.
- [43] J. L. Champeaux, P. O. Dupuy, I. Laurantin, P. Soulan, P. Tabary, and J. M. Soubeyrou, "Les mesures de précipitations et l'estimation des lames d'eau à Météo-France: état de l'art et perspectives," *La Houille Blanche*, vol. 5, pp. 28–34, 2009.
- [44] J. L. Champeaux, O. Laurantin, B. Mercier, F. Mounier, P. Lassegues, and P. Tabary, "Quantitative precipitation estimations using rain gauges and radar networks: inventory and prospects at Météo-France," 2011.
- [45] F. Fabry, G. L. Austin, and D. Tees, "The accuracy of rainfall estimates by radar as a function of range," *Quarterly Journal of the Royal Meteorological Society*, vol. 118, no. 505, pp. 435–453, 1992.
- [46] G. Delrieu, H. Andrieu, and J. D. Creutin, "Quantification of path-integrated attenuation for X- and C-band weather radar systems operating in mediterranean heavy rainfall," *Journal of Applied Meteorology*, vol. 39, no. 6, pp. 840–850, 2000.
- [47] D. N. Moriasi, J. G. Arnold, M. W. Van Liew, R. L. Bingner, R. D. Harmel, and T. L. Veith, "Model evaluation guidelines for systematic quantification of accuracy in watershed simulations," *Transactions of the ASABE*, vol. 50, no. 3, pp. 885–900, 2007.
- [48] W. F. Krajewski, G. Villarini, and J. A. Smith, "Radar-rainfall uncertainties: where are we after thirty years of effort," *Bulletin of the American Meteorological Society*, vol. 91, no. 1, pp. 87–94, 2010.
- [49] S. Sinclair and G. Pegram, "Combining radar and rain gauge rainfall estimates using conditional merging," *Atmospheric Science Letters*, vol. 6, no. 1, pp. 19–22, 2005.
- [50] M. Steiner, J. A. Smith, S. J. Burges, C. V. Alonso, and R. W. Darden, "Effect of bias adjustment and rain gauge data quality control on radar rainfall estimation," *Water Resources Research*, vol. 35, no. 8, pp. 2487–2503, 1999.



**Hindawi**

Submit your manuscripts at  
<http://www.hindawi.com>

